

## Additive-assisted oriented growth of cobalt oxide: controlled morphology and enhanced supercapacitor performance

Radhika S. Desai<sup>a</sup>, Vinayak S. Jadhav<sup>a</sup>, Sidharth R. Pardeshi<sup>b</sup>, Pramod S. Patil<sup>c,d</sup>, Rafe H. Mohammad<sup>e</sup>, Anil K. Yedluri<sup>f</sup>, Dhanaji S. Dalavi<sup>a\*</sup>

<sup>a</sup>Department of Physics, Krishna Mahavidyalaya, Rethare Bk, Post-Shivnagar, Tal- Karad, Dist. Satara 415108, Maharashtra, India.

<sup>b</sup>Department of Physics, Mahindra University, Hyderabad, India

<sup>c</sup>Department of Physics, Shivaji University, Kolhapur, 416004, India.

<sup>d</sup>National Dong Hwa University, Hualien, Taiwan.

<sup>e</sup>Department of Chemistry, College of Science, King Saud University, P.O. Box 2455, Riyadh 11451, Saudi Arabia

<sup>f</sup>Saveetha School of Engineering, Saveetha Institute of Medical and Technical Sciences, Saveetha University, Chennai 602105, Tamil Nadu, India.

\*E-mail: [dhanuphysics@gmail.com](mailto:dhanuphysics@gmail.com) (Dhanaji S. Dalavi)

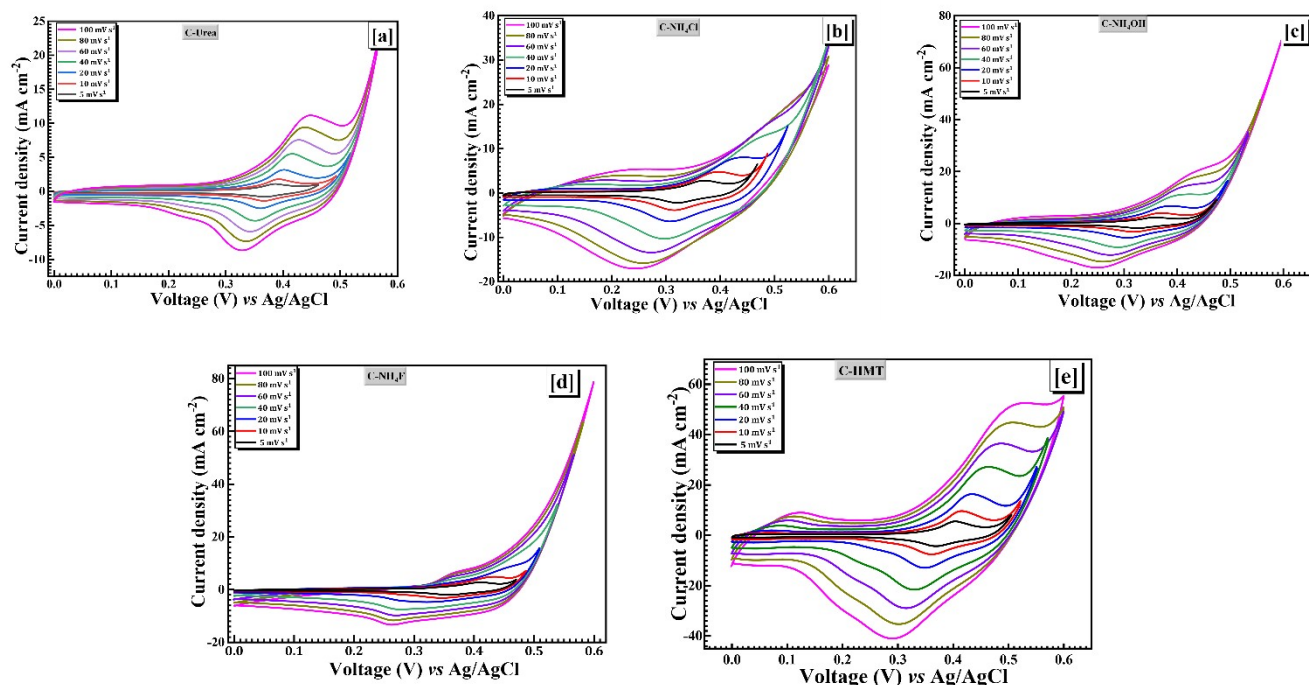


**Fig. S1** CV analysis data of (a) C-Urea (b) C-NH<sub>4</sub>Cl (c) C-NH<sub>4</sub>OH (d) C-NH<sub>4</sub>F and (e) C-HMT samples at different scan rates upon application of potential 0 to 0.6 V.

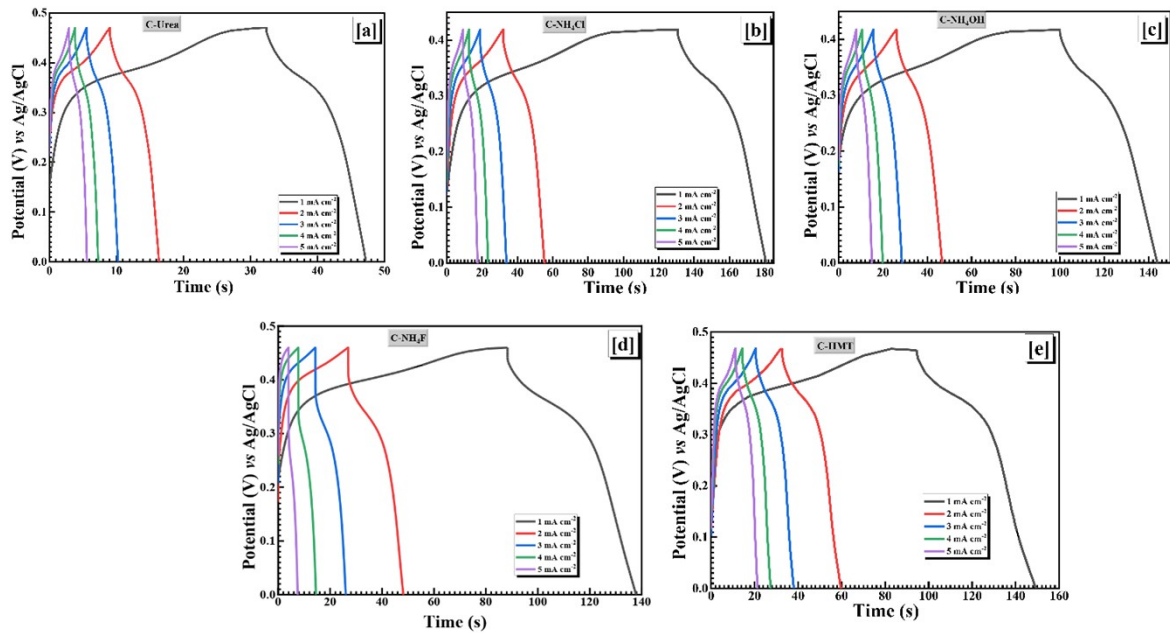


**Fig. S2** GCD analysis data of (a) C-Urea (b) C-NH<sub>4</sub>Cl (c) C- NH<sub>4</sub>OH (d) C-NH<sub>4</sub>F and (e) C-HMT samples at different current densities.

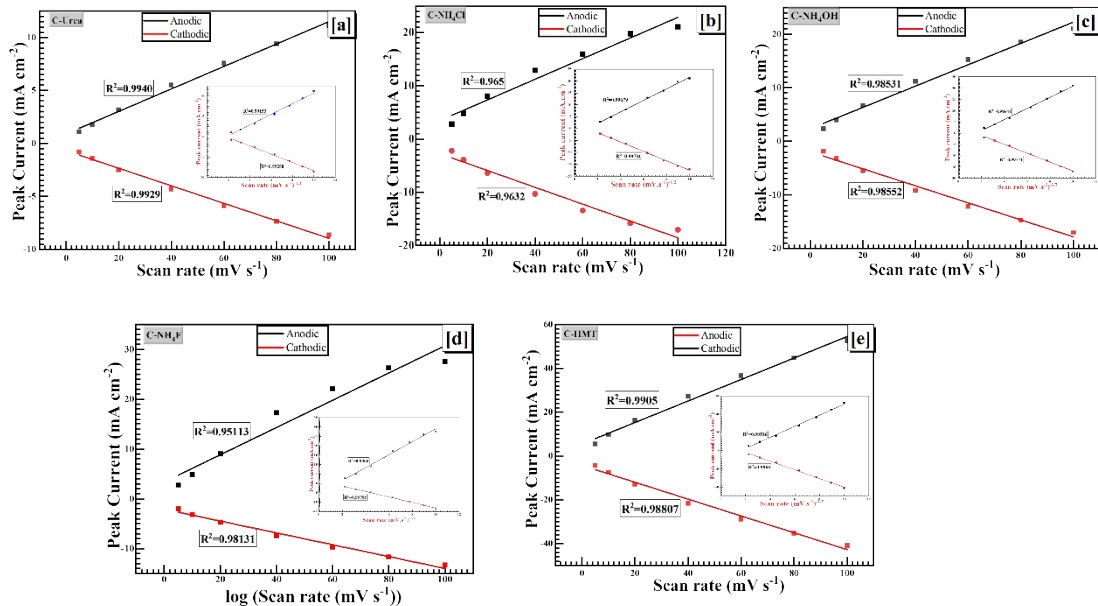


**Fig. S3** Dependence of redox peak current on the scan rate for the synthesized sample and inset redox peak current vs square root scan rate.

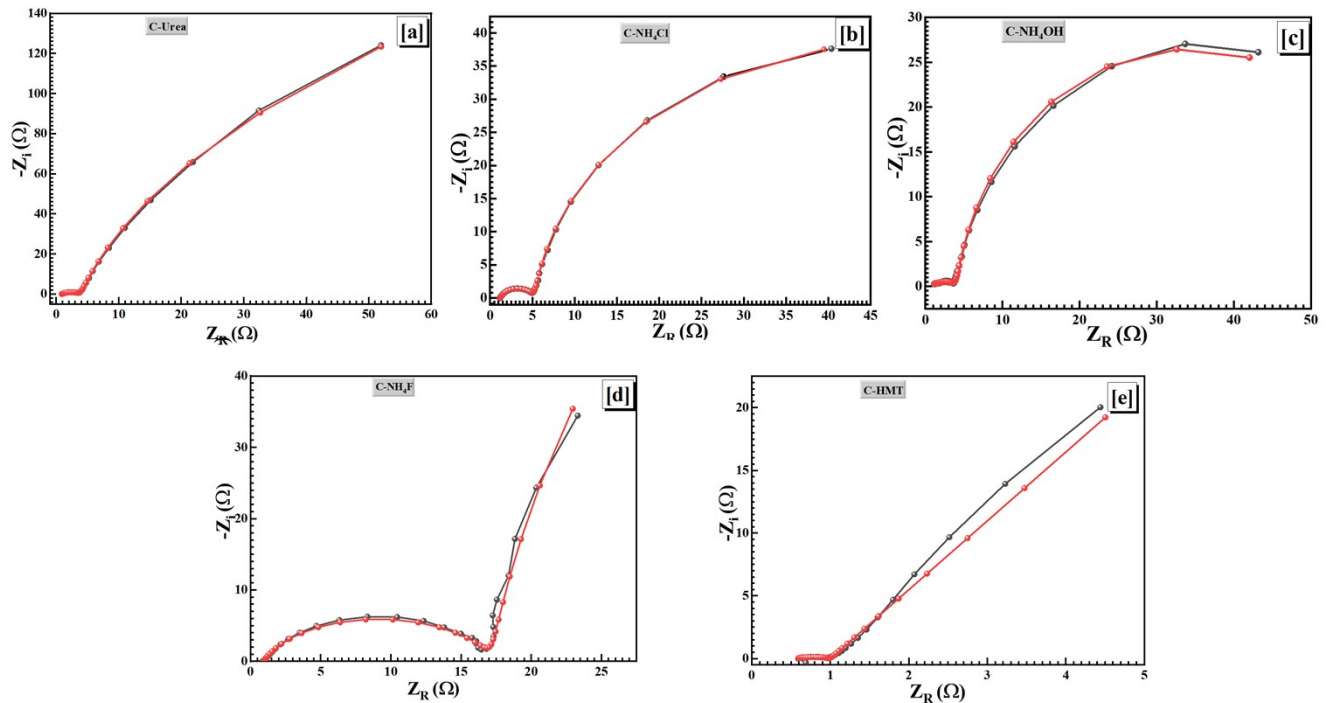


**Fig. S4** Nyquist plot of (a) C-Urea (b) C-NH<sub>4</sub>Cl (c) C-NH<sub>4</sub>OH (d)C-NH<sub>4</sub>F and (e) C- HMT samples

**Table S<sub>1</sub>** Analysis of CV measurements of all synthesized samples.

Samples Scan rate	C-Urea		C- NH <sub>4</sub> Cl		C- NH <sub>4</sub> OH		C- NH <sub>4</sub> F		C-HMT	
	Anodic peak current $i_{pa}$ (mA/cm <sup>2</sup> )	Cathodic peak current $i_{pc}$ (mA/cm <sup>2</sup> )	Anodic peak current $i_{pa}$ (mA/cm <sup>2</sup> )	Cathodic peak current $i_{pc}$ (mA/cm <sup>2</sup> )	Anodic peak current $i_{pa}$ (mA/cm <sup>2</sup> )	Cathodic peak current $i_{pc}$ (mA/cm <sup>2</sup> )	Anodic peak current $i_{pa}$ (mA/cm <sup>2</sup> )	Cathodic peak current $i_{pc}$ (mA/cm <sup>2</sup> )	Anodic peak current $i_{pa}$ (mA/cm <sup>2</sup> )	Cathodic peak current $i_{pc}$ (mA/cm <sup>2</sup> )
5 mV s <sup>-1</sup>	1.0999	-0.7944	2.8120	-2.2182	2.3246	-1.8353	2.7507	-1.9405	5.5345	-4.3018
10 mV s <sup>-1</sup>	1.7750	-1.3956	4.7834	-3.8716	3.9528	-3.2539	4.8647	-3.1554	9.6478	-7.5351
20 mV s <sup>-1</sup>	3.1762	-2.4856	8.0422	-6.3984	6.6847	-5.5391	9.0382	-4.7065	16.3281	-12.8885
40 mV s <sup>-1</sup>	5.5277	-4.3143	12.8688	-10.3023	11.2236	-9.1747	17.2542	-7.4926	27.1808	-21.5865
60 mV s <sup>-1</sup>	7.5811	-5.9031	15.9275	-13.4162	15.3020	-12.1580	22.0945	-9.7683	36.5024	-28.9577
80 mV s <sup>-1</sup>	9.4031	-7.3456	19.7650	-15.8179	18.5915	-14.7481	26.2622	-11.6597	44.8136	-35.2725
100 mV s <sup>-1</sup>	11.1593	-8.6544	21.0319	-17.0440	21.0559	-17.0293	27.5618	-13.3235	52.5287	-40.9790

**Table S2.** Literature data on pristine  $\text{Co}_3\text{O}_4$  thin film on a steel substrate.

Deposition technique	Morphology	Capacitance	Energy density, power density, and coulombic efficiency	Cycle stability	Electrolyte	Ref.
single-step solution precursor plasma spray route.	Nanoparticle (10–50 nm)	$\sim 162 \text{ F g}^{-1}$ at 2.75 $\text{A g}^{-1}$	-	72.2% after 1000 cycles	6 M KOH	[4]
Potentiodynamic electrodeposition method	nanoflakes	$365 \text{ F g}^{-1}$ at 5 $\text{mV s}^{-1}$ .	$64 \text{ Wh kg}^{-1}$ , $21.53 \text{ kW kg}^{-1}$ , and 99 %	92 % of initial capacity over 2,000 cycles	1M KOH	[5]
potentiodynamically synthesized cobalt oxide	agglomeration of granular micro-particles	$441.17 \text{ F g}^{-1}$ 2 $\text{mV s}^{-1}$	-	87.88% stability after 1000 cycles at 40 $\text{mA/cm}^2$ .	1 M KOH	[6]
low-temperature wet chemical synthesis strategy	nano-needles	$66.40 \text{ mAh g}^{-1}$ at 1 $\text{mA cm}^{-2}$	-	-	$\text{NaOH}$ , $\text{KOH}$ and $\text{Na}_2\text{SO}_4$	[7]
potentiostatically	nano-particles	$284.4 \text{ F g}^{-1}$ at 5 $\text{mV s}^{-1}$	$4.325 \text{ Wh kg}^{-1}$ , $3 \text{ kW kg}^{-1}$ , 53.75 %	-	1 M $\text{Na}_2\text{SO}_4$	[8]
Hydrothermal	urchin	$536 \text{ F g}^{-1}$ at 4 $\text{A g}^{-1}$		23% after 5000 charge-discharge cycles current density of $4 \text{ A g}^{-1}$	3 M KOH	[34]
Electrodeposition	nano-plates	$393.6 \text{ F g}^{-1}$ at 1 $\text{A g}^{-1}$		96.5% after 500 charge-discharge cycles	1 M KOH	[43]
Electrodeposition	nanoflakes	$315 \text{ F g}^{-1}$ at 5 $\text{mV s}^{-1}$			0.5 M $\text{Na}_2\text{SO}_4$	[44]
Hydrothermal	nanoflakes	$454 \text{ F g}^{-1}$ at 2 $\text{A g}^{-1}$		High capacitance retention after 2500 charge-discharge cycle	2 M KOH	[45]
Hydrothermal synthesis	Nanosheets	$468.68 \text{ F g}^{-1}$ at a 5 $\text{mV s}^{-1}$		98.31 % of its initial capacitance after 10000 cycles	2 M KOH	This work